Primary relaxation in a hard-sphere system

M. Fuchs, I. Hofacker, and A. Latz
Physik-Department, Technische Universität München, D-8046 Garching, Federal Republic of Germany
(Received 19 August 1991)

The α-relaxation dynamics in a hard-sphere system is studied solving microscopic-mode-coupling equations. The solutions for coherent and incoherent dynamical structure factors, the transversal correlation functions, and the moduli are presented for all wave vectors. The wave-vector dependence of fitted Kohlrausch exponents β and of the relaxation times τ is discussed. Recent experiments on the α relaxation of colloidal systems are quantitatively analyzed.

PACS number(s): 64.70.Pf, 61.20.Lc, 82.70.Dd

I. INTRODUCTION

The appearance of a slow structural relaxation process referred to as primary or α relaxation is a characteristic feature of supercooled liquids. Very often, but not always, the correlation function $\Phi_X(t)$ of some variable X can be written as

$$\Phi_X(t)=\hat{\Phi}_X(t/\tau) , \tag{1}$$

where the master function $\hat{\Phi}$ varies only smoothly with temperature, while the scale τ increases rapidly upon cooling. The master function $\hat{\Phi}_X$ depends on the variable X measured and is different for different glass-forming systems. An equivalent scaling law or time-temperature superposition principle holds for the susceptibility $\chi_X(z)$:

$$\chi_X(z)=\hat{\chi}_X(z\tau) , \quad \mathrm{Im}z>0 , \tag{2}$$

where the master function $\hat{\chi}_X(z\tau)$ is related to the Laplace transform $\Phi_X(z)$ via $z\Phi_X(z)+\Phi_X(t=0)=\chi_X(z)$. The spectrum $\chi''(\omega)$ exhibits an α resonance where the position shifts with temperature T proportional to $1/\tau$. Our paper deals with the detailed form of the master function $\hat{\Phi}_X(t/\tau)$ or the shape of the α peak $\hat{\chi}''_X(\omega\tau)$. One characteristic feature is the stretching: several decades in time t or frequency ω have to be mapped out in order to investigate the α relaxation. This was discovered by Kohlrausch in the last century who also proposed a simple fit formula

$$\hat{\Phi}_X(t)=f_X\exp[-(t/\tau)^{\beta}] . \tag{3}$$

The stretching is modeled by the Kohlrausch exponent $\beta<1$. Different physical quantities exhibit different β. There are also systematic deviations between true master functions and the Kohlrausch function. Experiments show that β and the correct form of $\hat{\Phi}$ or $\hat{\chi}$ depend on the microscopic details of the system. There is no universality. There is no fit formula known which accounts properly for all details of the master curve. There is no accepted microscopic or phenomenological theory for $\hat{\Phi}$. For more details we refer to some review, e.g., the book of Wong and Angell [1].

In recent years the mode-coupling theory (MCT) for supercooled liquid dynamics has been developed [2–5]. For some reviews the reader is referred to Refs. [6,7]. This approach aims at the evaluation of the relevant correlators of simple liquids focusing on two physical mechanisms: nonlinear coupling of density fluctuations and phonon-assisted hopping. The new results of the MCT are based on the existence of bifurcation singularities in the closed equations of motion [8]. These are referred to as glass-transition singularities. They separate ergodic liquid from nonergodic glassy states. The nonergodic state is characterized by a nonvanishing Edwards-Anderson parameter [9]. Neglecting hopping events, an ideal liquid-to-glass transition is obtained, if the temperature T crosses some critical value T_c or the density some critical density n_c. The existence of the temperature T_c lying above the calorimetric glass-transition temperature T_g is established in a number of glass-forming systems, e.g., Refs. 10–13. For some systems there are hints on the relevance of T_c [14–16]. In the limit $T\to T_c$, $T>T_c$, there appears an α process obeying (1), and a closed equation for the master functions $\hat{\Phi}_X$ is derived. In this manner the MCT provides a microscopic model, allowing, in principle, $\hat{\Phi}_X$ to be calculated. If hopping effects [17] or other ergodicity-restoring processes [5] are included the sharp transition is changed to a crossover. However, in a range of temperatures above T_c the mentioned idealized results are predicted to remain valid.

The functional form of the α master curve is predicted to depend on all microscopic details. Nevertheless, using simple schematic MCT models, already qualitative predictions about the shapes of α peaks are possible [18]. The α relaxation of real glass formers can only be calculated if the microscopic equations of the system are known. Up to now such equations exist only for simple one- and two-component liquids [3,19,20]. The first to solve the complete MCT equations at the glass transition for a simple one-atomic Lennard-Jones system was Bengtzelius [21]. However, he did not discuss the α master curves systematically nor could he study the adequacy of the Kohlrausch fits, which he showed for two wave vectors, because of complications due to β processes. The time scale of crystallization in one-atomic Lennard-Jones systems is much shorter than the α relaxation scale at T_c. Therefore, even on computers, it is very difficult to

supercool them for such long times to explore T_c effects.

In recent years an experimentally accessible system has been developed, which well corresponds to the most simple theoretical glass-forming liquid, the hard-sphere system (HSS). Suspensions of small colloidal spherical particles of equal size show structural and dynamical properties that have many features in common with those of simple atomic systems [22]. Especially, the interaction can be very short ranged and come close to one of an ideal HSS [23]. In contrast to simple one-atomic liquids a colloidal suspension can be brought to the metastable or glassy state for hours or days without crystallization. Recent dynamic light-scattering studies detected a glass transition at a critical packing fraction $\varphi_c = 0.560 \pm 0.005$ [24,25]. With a relative deviation of 7% this value is in agreement with computer simulations [26,27] and theoretical MCT calculations [3,28]. The MCT predicts a further slow relaxation process, the so-called β relaxation, to precede the α process. Very different from the α process the β process depends only on one single number λ, which combines all microscopic structural details. This exponent parameter λ can be calculated from microscopic models [29]. A rather detailed quantitative analysis of the β relaxation dynamics of the colloidal system [30] was possible using MCT predictions [31]. The results show that the MCT is a candidate for an adequate description of the colloidal HSS.

Also the α dynamics of a HSS is, in principle, accessible in colloidal suspensions. In this paper therefore a detailed analysis of the MCT predictions for the α relaxation of a HSS is given. Except for the first steps of Bengtzelius in this direction we are not aware of any microscopically based study of the α relaxation. The attempt of Ref. [32] to calculate the dynamics of a Lennard-Jones fluid using MCT equations could not extend the time window to more than three decades below the microscopic time scale. This is clearly inadequate for the analysis of α relaxation dynamics. In the present paper the wave vector and time dependence of the slowest relaxation process in a supercooled simple liquid are studied theoretically.

Our paper is organized as follows. In Sec. II we give a short summary of the MCT results for the α relaxation. Section III contains remarks about the numerical procedure and its accuracy. In Sec. IV we present the wave-vector-dependent solutions for the coherent and incoherent density fluctuations and the transverse shear correlators in the α relaxation regime. Different fit formulas and the recently proposed scaling procedure of Dixon *et al.* [33] are discussed. The theoretical results are compared with measurements on colloidal suspensions.

II. BASIC EQUATIONS

The normalized density correlation function $\Phi_q(t) = S(q,t)/S(q)$ can be rewritten in terms of a generalized longitudinal modulus $M_q(z)$:

$$\Phi_q(z) = \frac{-1}{z - \dfrac{\Omega_q^2}{z + M_q(z)}} \tag{4}$$

$$\Phi_q(z) = i \int_0^\infty dt\, e^{izt} \Phi_q(t) \quad \text{for } \mathrm{Im} z > 0 \,. \tag{5}$$

Ω_q is connected to the q-dependent generalization of the isothermal sound velocity $c_0(q) = \Omega_q/q = \sqrt{k_B T/(m S_q)}$ [34]. In the MCT of the glass transition the generalized longitudinal modulus $M_q(z)$ is approximated by pairs of density fluctuations [3]

$$M_q(z) = \Omega_q^2 m_q(z) + i \nu_q(z) q^2 \,, \tag{6}$$

$$m_q(t) = \tfrac{1}{2} \int \frac{d^3k}{(2\pi)^3} V(\mathbf{q},\mathbf{k}) \Phi_k(t) \Phi_{q-k}(t) \,, \tag{7}$$

$$V(\mathbf{q},\mathbf{k}) = n S_q S_k S_{q-k} \left[\frac{\mathbf{q}}{q} [\mathbf{k} c_k + (\mathbf{q}-\mathbf{k}) c_{q-k}] \right]^2 \Big/ q^2 \,. \tag{8}$$

c_q is the Ornstein-Zernicke direct correlation function and S_q is the static structure factor $S_q = 1/(1 - n c_q)$. Equations (4)–(8), or more precisely a quantum-mechanical generalization, were used earlier to describe the dynamics of liquid He II [35]. The term $i\nu_q(z)$ is a stochastic damping term, which is assumed to be frequency independent for $|z t_0| \ll 1$. t_0 characterizes microscopic time scales like inverse phonon frequencies. Equations (4)–(8) form a self-consistent set of equations for the description of the long-time dynamics of dense simple liquids close to the glass transition if the static structure factor S_q is known. Using Fokker-Planck equations as microscopics, Hess [36] has derived (4)–(7) and vertices slightly different from (8) for colloids also. The completely different microscopic behavior of colloids and pure HSS given by particle diffusion and hydrodynamic interaction enters only the term $i\nu_q(z)$. Even if one uses Smoluchowsky dynamics instead of Liouvillian dynamics it is possible to derive these equations for colloids if one neglects hydrodynamic interactions [37]. Equations (4)–(8) are the equations for the ideal glass transition. The influence of activated hopping or other ergodicity-restoring processes is not considered in this paper. These processes seem to have no influence on experiments in colloidal suspensions [30,31].

The α relaxation is asymptotically defined by the scaling limit $\varphi \to \varphi^c$, $z \to 0$, $\tau \to \infty$, $\hat{z} = z\tau = \text{const}$. τ is the scale of the α relaxation that goes to infinity if the packing fraction $\varphi = (\pi/6)\sigma^3 n$ of the hard-sphere system approaches some critical value φ^c, where σ is the diameter of the spheres. $\hat{\Phi}_q$ is the temperature independent master function obtained by the α scaling procedure. It obeys the following α scaling equation [38]

$$\hat{\Phi}_q(\hat{z}) = \frac{\hat{m}_q(\hat{z})}{1 - \hat{z}\hat{m}_q(\hat{z})} \,. \tag{9}$$

Here the vertices V in $\hat{m}_q(z)$ are evaluated at the critical point $\varphi = \varphi^c$. In time representation (9) can be written as [18]

$$\hat{\Phi}_q(\hat{t}) = \hat{m}_q(\hat{t}) - \frac{d}{d\hat{t}} \int_0^{\hat{t}} dt' \hat{m}_q(\hat{t} - t') \hat{\Phi}_q(t') \,, \quad \hat{t} = \frac{t}{\tau} \,. \tag{10}$$

The functions $\hat{\Phi},\hat{m}$ depending on the careted variables are related to the original ones via $\tau\hat{\Phi}_q(\hat{z})=\Phi_q(z)$, $\hat{\Phi}_q(\hat{t})=\Phi_q(t)$. In the following we discuss only the careted functions and drop the caret for convenience.

The scaling limit eliminates the microscopic and the intermediate β relaxation as transients to the α relaxation. The value of $\Phi_q(\hat{t}=0)=f_q$ is the strength of the α relaxation. From (9) one can derive the equation for f_q [3]:

$$\frac{f_q}{1-f_q}=m_q(\hat{t}=0)=\mathcal{F}_q(V,f_k)\ ,\quad 0\le f_q\le 1\ . \tag{11}$$

$\mathcal{F}$ is a functional of the function f_q determined by the vertices $V(\varphi)$ (8). The short-time expansion of (10) leads to [38]

$$\Phi_q(\hat{t})=f_q^c-h_q\hat{t}^b+h_q^{(2)}\hat{t}^{2b}-h_q^{(3)}\hat{t}^{3b}+O(\hat{t}^{4b})\ . \tag{12}$$

f_q^c is the value of f_q at the critical packing fraction φ^c. φ^c is defined by the occurrence of a fold bifurcation in Eq. (11) for f_q. The fractal short-time power behavior $\Phi_q(\hat{t})-f_q^c\propto\hat{t}^b$ is the so-called von Schweidler law. The von Schweidler exponent b is determined by the exponent parameter λ via $\Gamma^2(1+b)/\Gamma(1+2b)=\lambda$ [39]. Γ is the gamma function. The exponent parameter λ is defined by

$$\lambda=\int\frac{d^3q}{(2\pi)^3}\int\frac{d^3k}{(2\pi)^3}\hat{e}_q^c\frac{\partial^2\mathcal{F}_q}{\partial f_k\partial f_{q-k}}\times(1-f_k)^2(1-f_q)^2e_k^ce_{q-k}^c\ ,$$

$$0<\lambda<1\ . \tag{13}$$

The vectors $\hat{e}_q^c,e_q^c$ are appropriately normalized left and right eigenvectors of the stability matrix $C_{qk}=(\partial\mathcal{F}_q/\partial f_k)(1-f_k^c)^2$ at the critical packing fraction φ^c. The definition of φ^c above is equivalent to a nondegenerate maximal Eigenvalue $E=1$ of C_{qk}. The amplitude of the von Schweidler law h_q is equal to $h_q=(1-f_q^c)^2e_q^c$. λ also determines the critical variation of the α relaxation scale τ: $\tau\propto|\varphi-\varphi^c|^{-\gamma}$, where $\gamma=1/2a+1/2b$ depends on the von Schweidler exponent b and the positive solution a of $\Gamma^2(1-a)/\Gamma(1-2a)=\lambda$.

The α master curve of the self-correlation function $\Phi_q^s(\hat{t})$ is the solution of

$$q^2\Phi_q^s(\hat{t})=m_q^s(\hat{t})-\frac{d}{d\hat{t}}\int_0^{\hat{t}}dt'm_q^s(\hat{t}-t')\Phi_q^s(t')\ , \tag{14}$$

$$m_q^s(\hat{t})=\tfrac{1}{2}\int\frac{d^3k}{(2\pi)^3}V^s(\mathbf{q},\mathbf{k})\Phi_k(\hat{t})\Phi_{q-k}^s(\hat{t})\ , \tag{15}$$

$$V^s(\mathbf{q},\mathbf{k})=n\left[\frac{\mathbf{qk}}{q}\right]^2c_k^2S_k\ . \tag{16}$$

The coherent function $\Phi_q(\hat{t})$ is an input in the equations for $\Phi_q^s(\hat{t})$. As in the coherent case, the value $\Phi_q^s(\hat{t}=0)=f_q^s$ is a measure of the strength of the incoherent α process. It obeys

$$q^2\frac{f_q^s}{1-f_q^s}=m_q^s(f_k,f_{q-k}^s)\ ,\quad 0\le f_q^s\le 1\ . \tag{17}$$

The rescaled short-time expansion is given by

$$\Phi_q^s(\hat{t})=f_q^s-h_q^s\hat{t}^b+h_q^{s2}\hat{t}^{2b}-h_q^{s3}\hat{t}^{3b}+O(\hat{t}^{4b})\ . \tag{18}$$

The von Schweidler exponent b is the same as in (12).

Finally the time- and wave-vector-dependent transversal current relaxation kernel in the α regime is given by

$$m_q^t(\hat{t})=\tfrac{1}{2}\int\frac{d^3k}{(2\pi)^3}V^t(\mathbf{q},\mathbf{k})\Phi_k(\hat{t})\Phi_{q-k}(\hat{t})\ , \tag{19}$$

$$V^t(\mathbf{q},\mathbf{k})=nS_kS_{q-k}(c_k-c_{q-k})^2\left[k^2-\left[\frac{\mathbf{qk}}{q}\right]^2\right]\Big/q^2\ . \tag{20}$$

For the derivation of the above summarized formulas (9)–(20) the reader is referred to the original MCT papers [3,29,38,39] or to the review [6].

III. NUMERICAL PROCEDURES

Equations (4)–(8) specify a microscopic infinite-dimensional model for the α dynamics of a HSS. Numerically the wave-vector space has to be discretized and an upper cutoff $q_{\max}$ has to be introduced. The mesh size has to be small enough to resolve the central peak of S_q. $\Delta q=0.1/a$ was chosen. The length scale a is connected to the density by $(4\pi/3)a^3n=1$. The cutoff $q_{\max}=30/a$ ensures that the integrands of the wave-vector integrals in (7) are negligible for $q>q_{\max}$. A model of dimension $N=300$ is obtained. The Verlet-Weiss approximation [34] for the static structure of a HSS was used to calculate the vertices.

The result of the α relaxation strength f_q^c of this $N=300$ model can be compared to earlier calculations [3,27,32], see Fig. 1: For $qa>2.5$ good agreement is found except for the results of [32]. The Percus-Yevick approximation [34] for S_q used in [3] leads to smaller f_q^c for $qa<2.5$. This difference lies beyond numerical er-

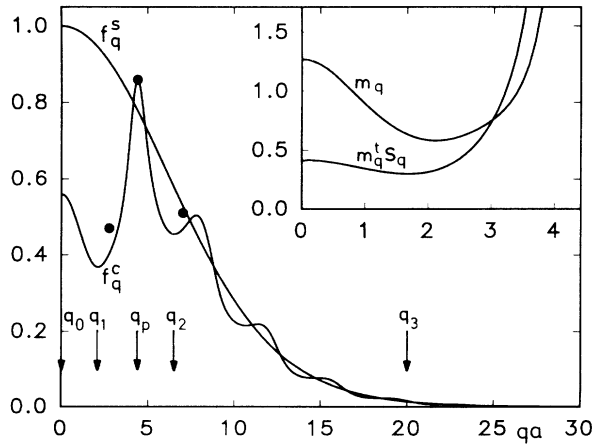

FIG. 1. Coherent and incoherent α relaxation strengths f_q^c and f_q^s at the critical packing fraction $\varphi^c=0.525$. Three values for f_q^c from experiments on colloidal suspensions at volume fraction $\varphi_{\text{expt}}=0.565$ ($\varphi_{\text{expt}}=0.560$) from Ref. [25] are included. Five wave vectors, for which dynamical results are presented in more detail, are marked. The inset compares the small-q dispersion of the high-frequency transverse $[c_\infty^t(q)]^2=M_0S_qm_q^t(\hat{t}=0)$ and longitudinal $[c_\infty^l(q)]^2=M_0m_q(\hat{t}=0)$ sound velocity.

rors. Numerical errors in the wave-vector integration, however, are largest for small q due to cancellation effects. The errors can be estimated by comparing results of different algorithms. Differences for $qa<1$ and smaller than 10% errors at $q=0$ are seen compared to the results of Ref. [27]. Three experimentally obtained values for f_q^c [25] are also included in Fig. 1 and compare well to the theoretical results. The further unphysical wiggles observed in f_q^c of Ref. [32] are possibly caused by using a too small cutoff for the wave vectors ($q_{\max}=15.5/a$), where the integrands are not yet small.

The critical packing fraction of the $N=300$ model $\varphi^c=0.525$, which agrees with earlier calculations [21,27], lies below the experimental value $\varphi^c=0.560$ [24,25]. Generally it has been found that MCT overestimates the trend to freezing [17]. When comparing to experiments it is therefore necessary to use the distance to the transition points as a relevant parameter. The maximal *eigenvalue* of the stability matrix C_{qk} was $E=1\pm10^{-3}$ at φ^c. The result of Fig. 1 agree with the exact results of f_q^c of the discretized model up to relative errors of 0.5%. The model has an exponent parameter $\lambda=0.766(1\pm10^{-3})$, which is calculated from Eq. (13). The corresponding von Schweidler exponent b equals 0.532. The exponent γ, which describes the critical variation of the α-scaling time, with φ going to φ^c from below, is $\gamma=2.62$. This value has been checked in context with the already mentioned β-dynamics analysis of colloidal suspensions [31]. The value of $\tilde{\gamma}=2.0$ arbitrarily fitted in Ref. [32] to numerical data for shear and longitudinal viscosities of a HSS violates the exact relation $\gamma=1/2a+1/2b$.

A recently developed algorithm for integrating (10) [18] is used. The results of the integration in time space can be checked with Eq. (9) in Fourier space. The errors, largest at high frequencies, are mainly due to the Fourier transformation. They are at most 1.5% in $\Phi_q''(\omega)$ at the peak of the structure factor $q=q_p$ and 2% in $\Phi_q''^s(\omega)$ at $q=2.1/a$. For $qa<2.1$, $\Phi_q^s(t)$ decays too slowly, so that a reliable Fourier transformation is not possible. The peak positions and widths of the α peaks in the susceptibilities $\chi_q''^s(\omega)$, however, could be determined for $qa\geq1.5$. The numerical integration of (10) starting from $\hat{t}=10^{-3}$ to $\hat{t}=10^3$ took less than 20 min on a Cray Y-MP.

IV. RESULTS

The results for f_q^c and f_q^s also determine the high-frequency values of the transverse $M_q^t(\hat{t}=0)$ and tagged particle $M_q^s(\hat{t}=0)$ memory kernels. The transverse-high-frequency modulus $G_\infty=\lim_{q\to0}M_q^t(\hat{t}=0)/q^2$ is found to be $G_\infty/M_0=S_{q=0}m_{q=0}^t(\hat{t}=0)=0.41$, where $M_0=mnc_0^2$ is the thermodynamic bulk modulus. The high-frequency longitudinal sound velocity $[c_\infty^l(q)]^2=c_0^2m_q(\hat{t}=0)$ shows a stronger q-dependent dispersion than the corresponding transverse velocity, see Fig. 1. The q range of validity of the hydrodynamics is of the order of magnitude of the peak width in S_q, as has been discussed in Ref. [3]. The value $m_q^s(\hat{t}=0)=77.7=a^2/r_s^2$ gives a root-mean-square displacement $(\langle\Delta r_s^2\rangle)^{1/2}=\sqrt{2}r_s=0.1\sigma$, which can also be read off from f_q^s [3]. This shows that, for $qa<10$, f_q^s closely follows the Gaussian distribution $f_q^s=\exp(-q^2r_s^2)$. The value $(\langle\Delta r_s^2\rangle)^{1/2}=0.1\sigma$ corresponds to the Lindemann criterion of melting [34].

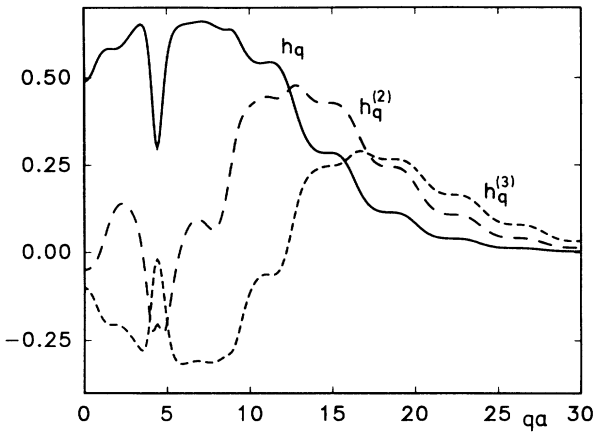

FIG. 2. Critical amplitude h_q^c and next two coefficients h_q^2,h_q^3 of expansion (12) of $\Phi_q(\hat{t})$ for $t/\tau\to0$.

The short-time von Schweidler law $\Phi_q(\hat{t}\to0)=f_q^c-h_q\hat{t}^b$ is the only simple analytic prediction of the MCT for the shape of the α relaxation. The correction terms $h_q^{(2)},h_q^{(3)}$ and h_q^{s2},h_q^{s3}, however, are of the same order of magnitude as the critical amplitudes h_q,h_q^s (see Figs. 2 and 3). Therefore, in general, the von Schweidler asymptote can be expected to hold only for short times, $\hat{t}\leq10^{-2}$, say. The exceptions are cases where $h_q^{(2)},h_q^{(3)}$ are either very small or where they are of the same size and nearly cancel each other.

Figure 4 shows normalized results $\Phi_q(\hat{t})/f_q^c$ for different wave vectors. In order to discuss the results and to show all possible features the correlators at $qa=0$, 2.2, 4.4, 6.5, and 20 were chosen. $q=q_p=4.4/a$ is the position of the principal peak of S_q and consequently of f_q^c. $q=q_1=2.1/a$ lies in the first minimum, and

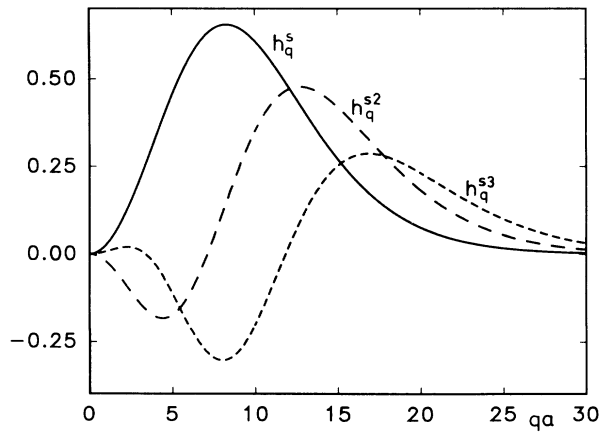

FIG 3. Critical amplitude h_q^s and next two coefficients h_q^{s2},h_q^{s3} of expansion (18) of $\Phi_q^s(\hat{t})$ for $t/\tau\to0$.

$q=q_2=6.5/a$ in the second minimum of f_q^c. $q=q_0=0$ and $q=q_3=20/a$ are typical results for $qa \ll 1$ and $qa \gg 1$, respectively. The results $\Phi_q(\hat{t})$ clearly cannot be described with exponential decay. This is mainly due to the short-time fractal time behavior [see also $\chi_q''(\hat{\omega})$ below]. The shape of the relaxation curve and the relative relaxation time $\hat{\tau}_q=\tau_q/\tau$ depend on q. The correlator at the structure peak $q=q_p$ has the longest relaxation

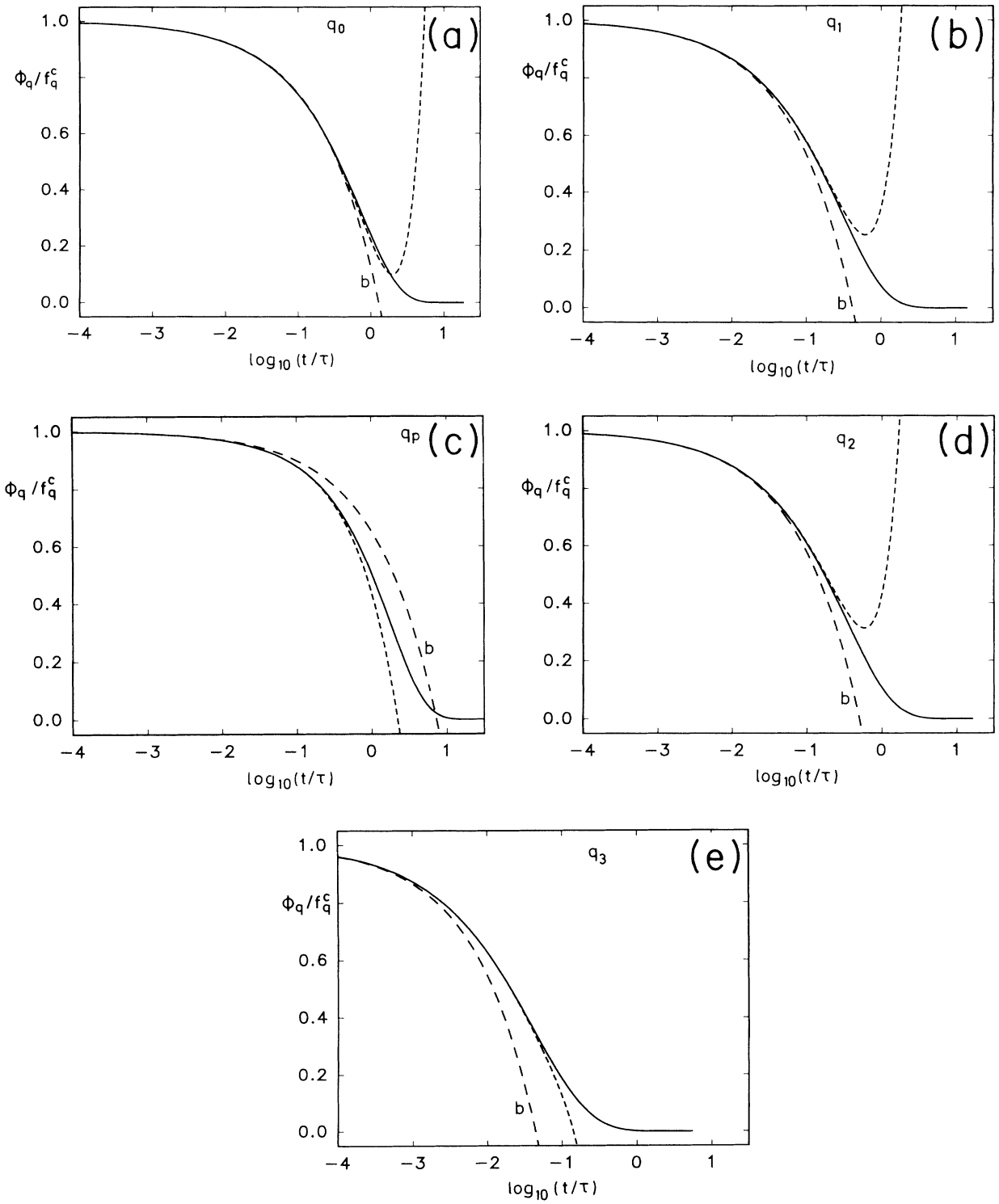

FIG. 4. (a) Normalized correlator $\Phi_q(\hat{t})/f_q^c$ for $q=q_0=0$ shown as solid line. The von Schweidler asymptote (marked with *b*) and the expansion (12) up to $\hat{t}^{3b}$ (short dashes) are also included. (b) Same as (a) for $q=q_1=2.1/a$ in the first minimum of f_q^c. (c) For $q=q_p=4.4/a$ at the structure peak in S_q and f_q^c. (d) For $q=q_2=6.5/a$ in the second minimum of f_q^c. (e) For $q=q_3=20./a$ at large q.

time but the smallest stretching. The opposite holds for $qa=20$. The von Schweidler asymptote and its corrections are also included in Fig. 4. The asymptote describes the decay only for $t/\tau \leq 10^{-2}$, except for $q=0$, where the corrections almost cancel. Figure 5 exemplifies this for $q=q_p$ in a double logarithmic plot. Having in mind experimental tests of the theory it is interesting to note that a fitted von Schweidler law with $\tilde{b}=0.565$, however, can reproduce the correlator even for times $t/\tau \approx 1$ within reasonable error bounds. This fit is also included in Fig. 5. A somewhat larger value of the critical amplitude $\tilde{h}_q=0.4$, instead of $h_q=0.3$, compensates for the small error in $\tilde{b}$. Figure 6 shows the results $\Phi_q^s(\hat{t})/f_q^s$ for the same wave vectors as in Fig. 4, except for the constant $\Phi_{q=0}^s(\hat{t})=1$. Again, differently, strong stretching and strongly varying relaxation times are obtained. In $\Phi_q^s(\hat{t})$ the von Schweidler asymptote is again seen only at short times except for $qa \approx 6.5$ where the corrections h_q^{s2}, h_q^{s3} nearly cancel.

The information concerning the relaxation times, line shapes, and the von Schweidler asymptote can also be discussed in the susceptibilities $\chi_q''(\omega)$ and $\chi_q''^s(\hat{\omega})$ (see. Figs. 7–9). The conjecture [17,40,18] that $\chi_q''(\hat{\omega})$ allows a momentum expansion $\chi_q''(\hat{\omega})=f_q^c c_q^0 \hat{\omega}[1+\delta(\hat{\omega})]$, where $\lim_{\hat{\omega}\to 0}\delta(\hat{\omega})=0$, is numerically verified. The Debye fits to the low-frequency side $\omega\tau \ll 1$ indicate that there is no anomalous stretching of the α relaxation for $\omega\tau \ll 1$. The Debye fits, where the slope and the peak height were adjusted, in general fail to reproduce the area of the α peak, i.e., the relaxation strength f_q^c. A double-logarithmic plot (Fig. 9) of the susceptibility at $q=q_p$ shows the validity of the $\propto \omega^1$ low-frequency asymptote. Whereas the Debye fit in general works for $\omega\tau < 10^{-1}$ only, at $q=q_p$ it fits the narrow peak up to $\omega\tau \approx 1$.

The frequency windows where the von Schweidler high- or the Debye low-frequency asymptotes are observed in $\chi_q''(\hat{\omega})$ are not in any obvious way connected to the corresponding regimes in the modulus. For $q=0$, $\hat{\omega}m_q''(\hat{\omega})$ is close to the von Schweidler asymptote, only for much higher frequencies than $\chi_q''(\hat{\omega})$ [compare Figs. 7(a) and 10].

The q-dependent stretching shows up in the varying width of the α peak in the susceptibilities. w_q shall denote the full width at half maximum measured in decades of $(\omega\tau)$. In $\chi_q''(\hat{\omega})$ and $\chi_q''^s(\hat{\omega})$ a general trend of increasing w_q with increasing q is found, see Fig.s 11 and 12. In $\chi_q''(\hat{\omega})$ a strong variation roughly in phase with the α relaxation strength f_q^c is superimposed on this trend, as suggested in Ref. [41]. The width varies rapidly around the peak of S_q at $q=q_p$. Another measure of the stretching of the α relaxation is the normalized slope of the correlator $\Sigma_q=(\partial\Phi_q(t)/\partial \ln\hat{t})|_{t=\tau_q^\Sigma}/\Phi_q(\tau_q^\Sigma)$ at the point of inflection $t=\tau_q^\Sigma$ where $\partial^2\Phi_q(t)/(\partial \ln t)^2=0$; this will be discussed below in context with the Kohlrausch-fit formula. w_q measures the stretching also for times preceding τ_q^Σ, where the slow von Schweidler time dependence still prevails. Σ_q therefore reflects less stretching than w_q, as can be seen in Fig. 11.

A very different variation of w_q with q happens in the memory kernels (see Fig. 13). The width of the α peaks in $\hat{\omega}m_q''(\hat{\omega})$, $\hat{\omega}m_q''^s(\hat{\omega})$, and $\hat{\omega}m_q''^t(\hat{\omega})$ varies only a little, about an average of $w_q \approx 1.9 \pm 0.13$. This common feature of the memory kernels and the value $w \approx 1.9$ are not obviously connected to the width of the corresponding susceptibilities.

In general the peak positions ω_q^p defined by $\chi_q''(\omega=\hat{\omega}_q^p)=(\chi_q'')_{\max}$ in the susceptibilities or generalized viscosities shift to higher frequencies with increasing wave vector. In the memory kernels a rather smooth change by a little more than one decade is observed in the whole q range (Fig. 13). Due to the hydrodynamic pole the peak positions cannot be determined for $qa < 1.5$ in $\chi_q''^s(\hat{\omega})$. From $qa=1.5$ to 30 the peak positions shift

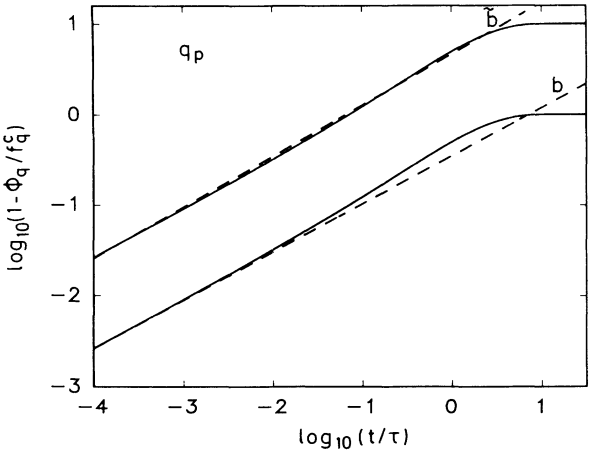

FIG. 5. Logarithmic plot of $1-\Phi_q(\hat{t})/f_q^c$ for $q=q_p$ vs logarithm of t/τ. The von Schweidler asymptote (marked with b) is shown; $b=0.532$ and $h_q=0.30$. With a vertical offset of one decade $\Phi_q(\hat{t})$ for $q=q_p$ is compared to a fitted von Schweidler law with $\tilde{b}=0.565$ and fitted critical amplitude $\tilde{h}_q=0.4$.

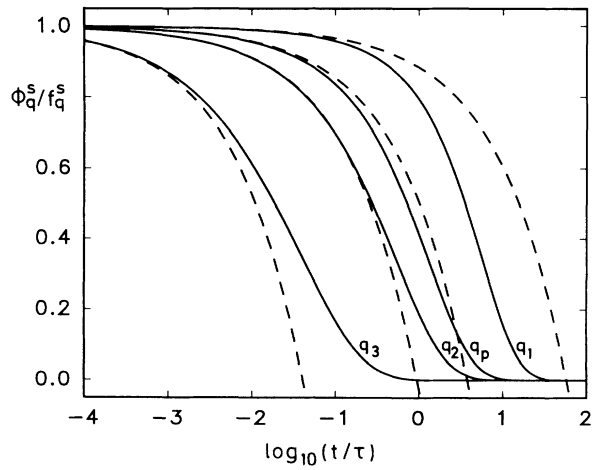

FIG. 6. Normalized tagged correlator $\Phi_q^s(\hat{t})$ for the wave vectors $q=q_1$, q_p, q_2, and q_3 from right to left. The von Schweidler asymptotes are shown as dashed curves.

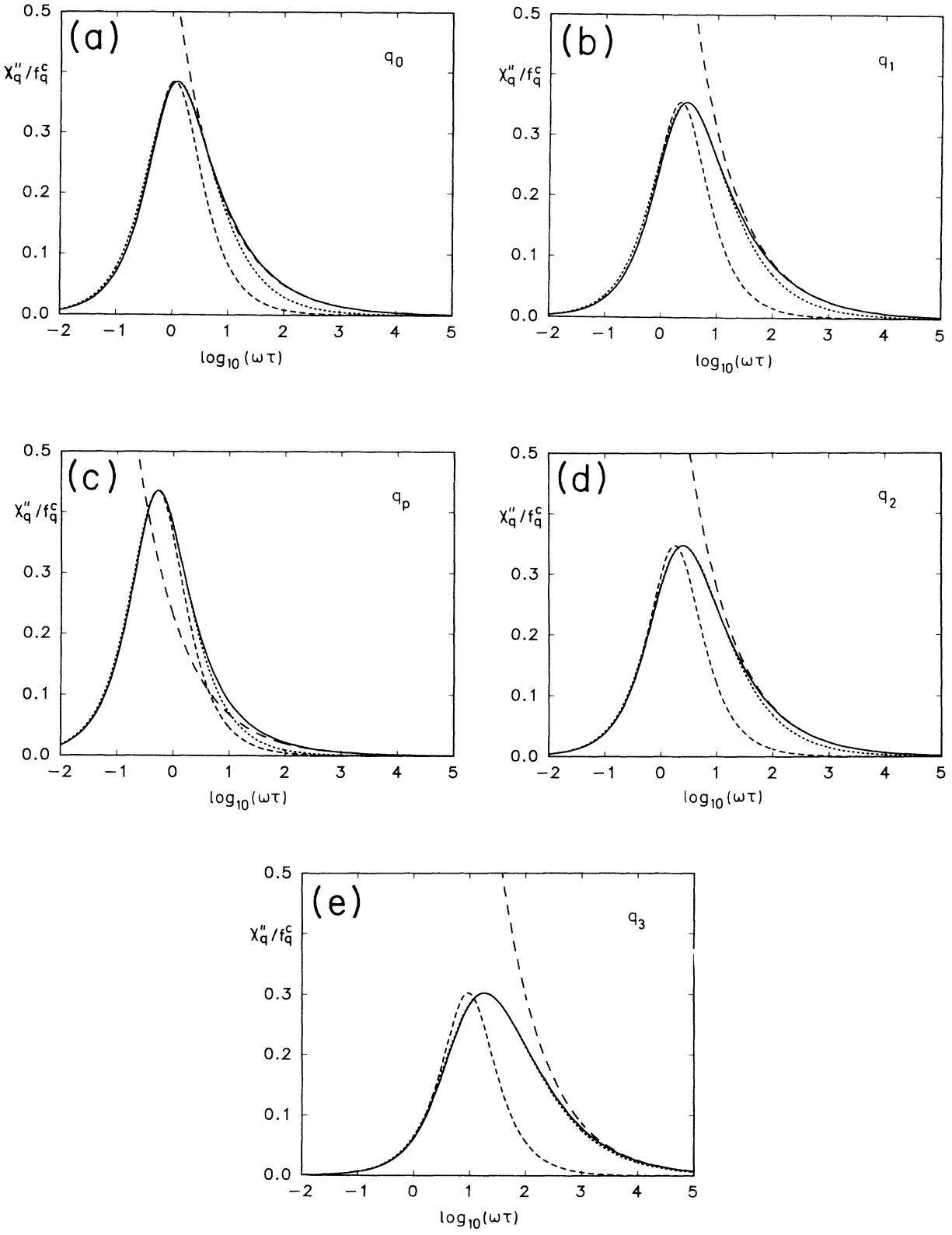

FIG. 7. Normalized susceptibility $\chi_q''(\hat{\omega})/f_q^c$ for wave vector $q=0$. A Debye law (short dashes) fitted to the low-frequency side $\omega\tau \ll 1$ and the von Schweidler asymptote (long dashes) for $\omega\tau \gg 1$ are included. A Kohlrausch law fitted to χ_q'' is shown as a dotted curve. The fitted Kohlrausch parameter is $\beta_{q_0}=0.77$. (b) Same as (a) for wave vector $q=q_1=2.1/a$. The Kohlrausch parameter $\beta_{q_1}=0.69$ was fitted. (c) For wave vector $q=q_p$ at the peak of S_q. A Kohlrausch fit with parameter $\beta_{q_p}=0.89$ is shown. (d) For wave vector $q=q_2=6.5/a$, $\beta_{q_2}=0.67$ is fitted. (e) For wave vector $q=q_3=20/a$, where the Kohlrausch fit gives $\beta_{q_3}=0.56$.

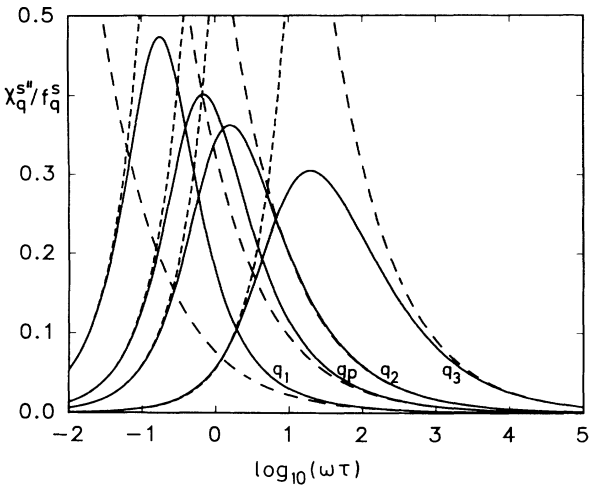

FIG. 8. Normalized tagged-particle susceptibilities $\chi_q''^s(\hat{\omega})/f_q^s$ for the wave vectors $q=q_1$, q_p, q_2, and q_3 from left to right. The von Schweidler high-frequency asymptotes (long dashes) and low-frequency fits linear in ω (short dashes) are included.

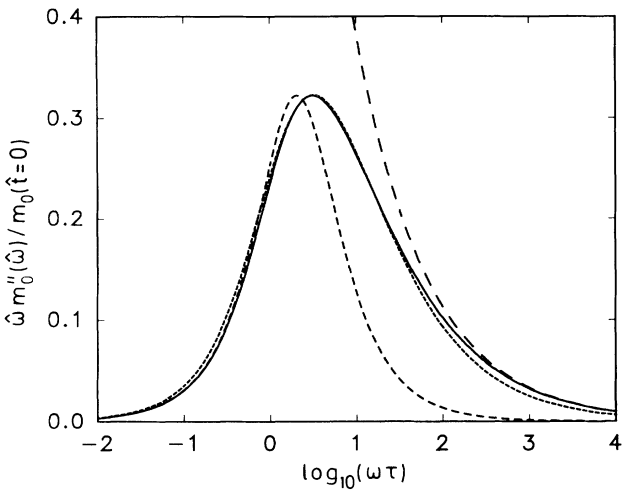

FIG. 10. Normalized longitudinal modulus $\hat{\omega}m_q''(\hat{\omega})/m_q(\hat{t}=0)$ at $q=0$. The von Schweidler high-frequency asymptote (long dashes) and a Debye fit to the low-frequency wing (short dashes) are included. A Kohlrausch fit to the whole α peak is also shown as dotted curve; the fitting procedure specified in the text leads to the following Kohlrausch parameters: $\beta=0.61$, $\tau^K=0.25$, and $f^K=0.98m_q(\hat{t}=0)$.

monotonically by more than 2.5 decades, see Fig 12. In $\chi_q''(\omega)$ the variation of ω_q^p also covers two decades. It is in phase with f_q^c and rather rapid around the primary peak $q=q_p$. The peak of $qa=2.1$ in the first minimum of f_q^c and the peak at $q=q_p$ are shifted by almost one decade relative to each other (Fig. 11). Two relaxation times can be obtained from the correlators directly. The already-mentioned τ_q^Σ of the point of inflection and an averaged relaxation time $\langle\tau_q\rangle=\int_0^\infty dt\,\Phi_q(t)/\Phi_q(t/\tau\to 0)$. This averaged time of the shear memory kernel, for example, connects shear-viscosity and high-frequency transverse modulus $\langle\tau^t\rangle=\eta^s/G_\infty$. The inverse of these relaxation times is included in Fig. 11. It is interesting to note that the self-motion relaxation time $\langle\tau_q^s\rangle$ varies proportionally to $1/q^2$ rather well for the whole wave-vector range $1.5\le qa\le 30$. The product $\langle\tau_q^s\rangle q^2=24\pm1.8$ shows only small but systematic wave-vector dependence. Somewhat larger variation by at most 17% is found for the corresponding product using the peak position ω_q^p in χ''^s.

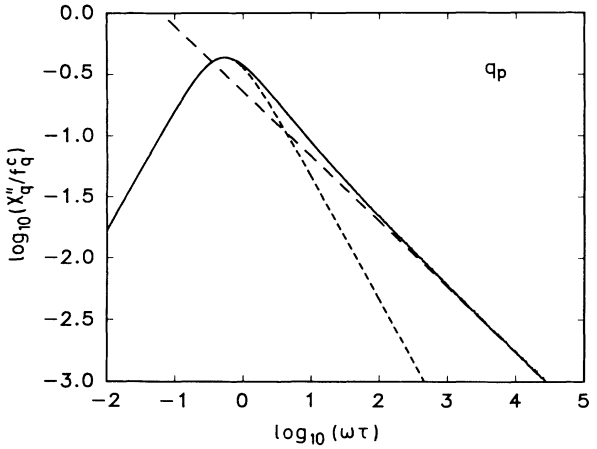

FIG. 9. Double-logarithmic plot of the normalized susceptibility $\chi_q''(\hat{\omega})/f_q^c$ at $q=q_p$. The Debye low-frequency (short dashes) and the von Schweidler high-frequency asymptotes (long dashes) are shown.

The transverse modulus $G(\hat{\omega})=(kT/m)\hat{\omega}m_{q=0}''^t(\hat{\omega})$ shown in Fig. 14 has a width of 1.8 decades. From its low-frequency slope the shear viscosity $\eta_s=nkTm_{q=0}''^t(\hat{\omega}=0)\,\tau=nkT\,19.23\tau$ can be read off. It is smaller than the longitudinal viscosity $\eta_l=\frac{4}{3}\eta_s+\eta_V=nkTm_{q=0}''(\hat{\omega}=0)/S_{q=0}\tau=nkT59.8\tau$ by a factor of 3.2. The self-motion memory kernel $M_q^s(z)=(kT/m)m_q^s(z)$ at $q=0$ determines the frequency-dependent self-diffusion function $D^s(\hat{\omega})$ via $D^s(\hat{\omega})=\mathrm{Im}[(kTm)/M_{q=0}^s(\hat{z}=\hat{\omega}+i0)]$. For $\omega\tau<1$ the rather constant value $D^s=(a^2/\tau)0.045$ is obtained. For $\omega\tau>1$, $D^s(\hat{\omega})$ diverges proportionally to $\hat{\omega}^{1-b}$, see Fig. 15. The time scale τ was reintroduced into the equations for η_s and D^s for clarity. The Stokes-Einstein relation [34] $D^s\eta_s=kT/6\pi R$ holds with $R=0.53\sigma$.

The exposition of the results for the α relaxation is complicated by the lack of exact analytical expressions. Phenomenologically different fit formulas have been used to describe the α relaxation. It is well known that no simple fit formula can describe the α dynamics in general. Fit formulas like the Cole-Cole law $\chi^{CC}(z)=\chi_0/[1+(-iz\tau)^\alpha]$, which assume a fractal frequency variation also for $\omega\tau<1$, clearly cannot describe the asymmetric results where $\chi''\propto\omega$ for $\omega\tau\ll1$ is found. The Kohlrausch law $\Phi^K(t)=f^K\exp[-(t/\tau^K)^\beta]$ [1] is widely used as a fit formula. This law plays a special role

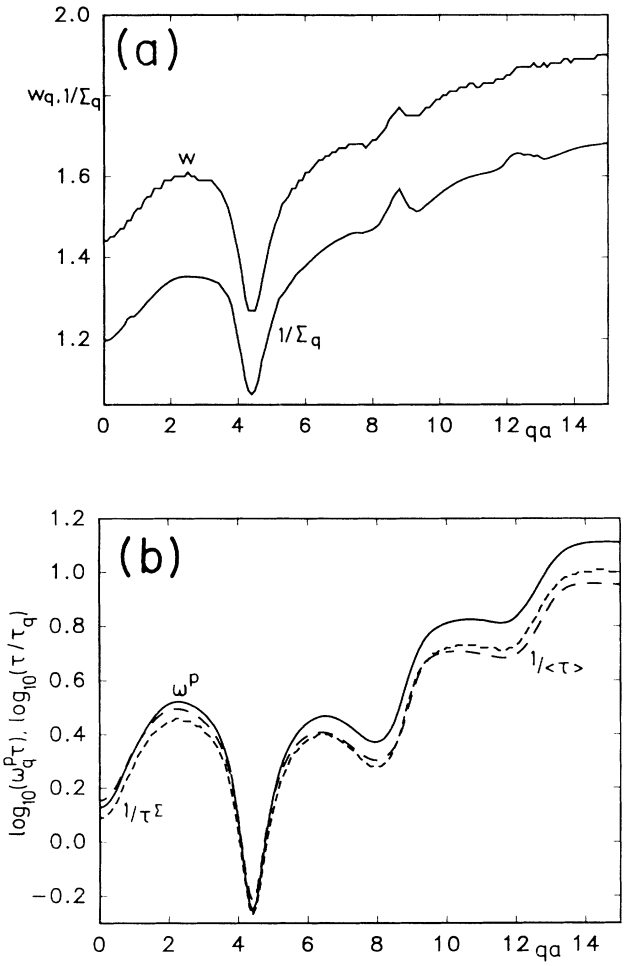

FIG. 11. (a) Stretching parameters obtained for the coherent density fluctuations. The full width at half maximum w_q measured in decades of $\omega\tau$ and the inverse of the normalized slope Σ_q obtained from the point of inflection in $\Phi_q(\hat{t})$ are shown. (b) Peak-shift parameters for the coherent density fluctuations: logarithmic plots of the peak position $\omega_q^p\tau$ in $\chi_q''(\hat{\omega})$ and of the inverse of the scaled relaxation times τ_q^Σ/τ and $\langle\tau_q\rangle/\tau$ are shown.

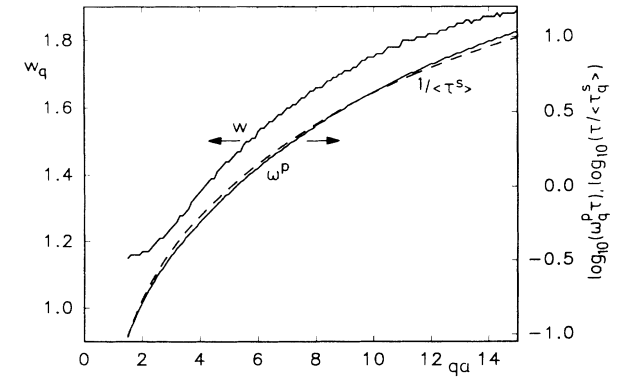

FIG. 12. Peak-shift and stretching parameters for the tagged-particle susceptibilities $\chi_q''^s(\hat{\omega})$. The full width at half maximum w_q in decades of $\omega\tau$ and a logarithmic plot of the peak position $\omega_q^p\tau$ and of the inverse of the scaled averaged relaxation time $\langle\tau_{q_s}\rangle/\tau$ are shown.

in the theory of limit distributions of random variables [42,43]. Applying the generalized central limit theorem to statistically independent correlators, all showing the same short-time von Schweidler asymptote, leads to a correlator where the Kohlrausch law is valid for all times [42]. The Kohlrausch exponent β in this case equals the von Schweidler exponent b.

Experimentally the α relaxation can always be studied on a finite-frequency window only. Least-squares fitting procedures of the Kohlrausch law to the α decay, in general, depend on the specified window. In order to remove this ambiguity, the following fitting procedure is used: The Kohlrausch parameter β is calculated from the full width at half maximum w_q of the peak in $\chi_q''(\hat{\omega})$ in decades of $\omega\tau$. The relation $\beta=\alpha_1/w_q+\alpha_2+\alpha_3 w_q$, where $\alpha_1=1.340$, $\alpha_2=-0.2463$, and $\alpha_3=6.237\times10^{-2}$, holds with less than 1% error in the range $0.5\le\beta\le1$. The peak position ω^p determines the relaxation time via

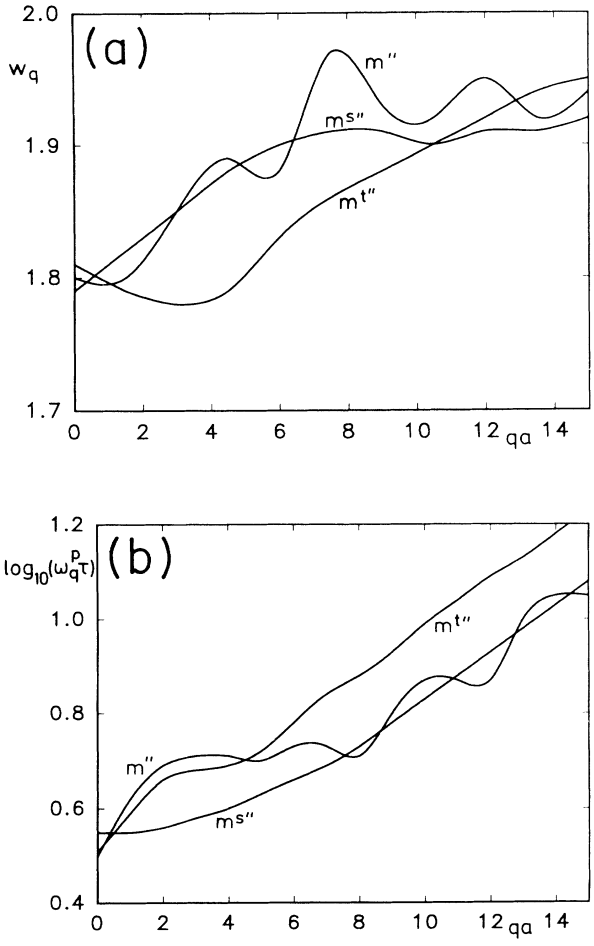

FIG. 13. (a) Stretching parameters for the normalized coherent m_q, incoherent m_q^s, and transverse m_q^t memory functions: the full widths at half maximum w_q in $\hat{\omega}m_q''(\hat{\omega})$, $\hat{\omega}m_q''^s(\hat{\omega})$, and $\hat{\omega}m_q''^t(\hat{\omega})$ are shown in units of decades of $\omega\tau$. (b) Peak-shift parameters for the memory functions of (a): logarithmic plots of the peak positions $\omega_q^p\tau$ in the specified moduli are shown.

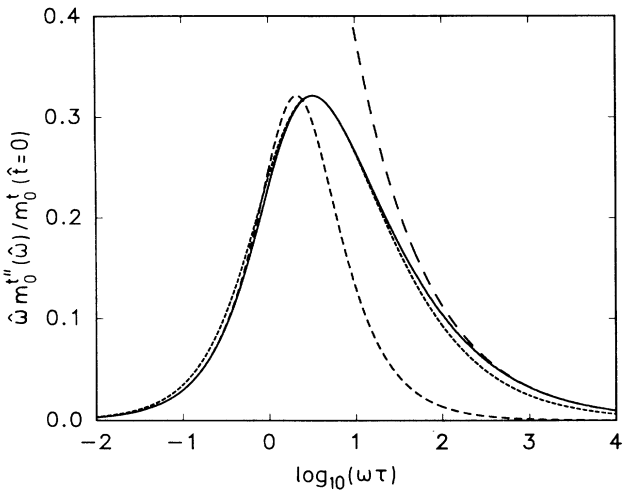

FIG. 14. Normalized transverse modulus $\hat{\omega} m_q''^t(\hat{\omega})/m_q^t(t=0)$ at $q=0$. The von Schweidler high-frequency asymptote (long dashes) and a Debye fit to the low-frequency wing (short dashes) are included. A Kohlrausch fit to the whole α peak is also shown as dotted curve; the fitting procedure to the peak specified in the text leads to the following Kohlrausch parameters: $\beta=0.61$ $\tau^K=0.24$, and $f^K=0.98 m_q^t(\hat{t}=0)$.

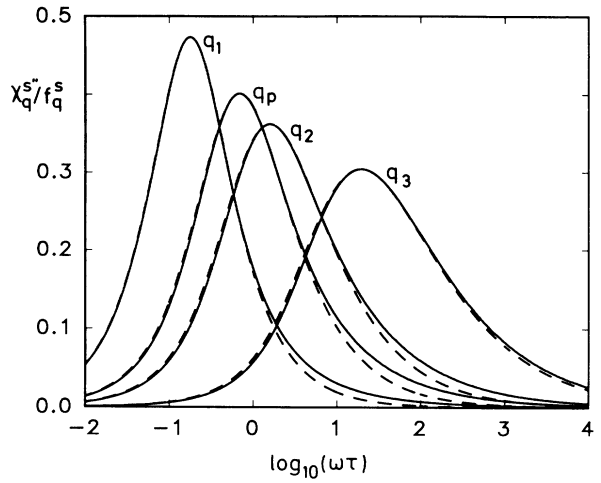

FIG. 16. Normalized tagged-particle susceptibilities $\chi_q''^s(\hat{\omega})/f_q^s$ compared to Kohlrausch fits to the peak position, width, and height. The curves from left to right correspond to the wave vectors $q=q$, q_p, q_2, and q_3.

$\omega^p\tau^K\approx 1$. The amplitude f^K can be taken from the height of the α peak in the susceptibility $f^K\approx\chi_{\max}$. In order to calculate $\tau^K=\tau^K(\omega_q^p)$, β-dependent corrections are necessary, because for a normalized Kohlrausch law, $\exp[-(t/\tau)^\beta]$, already ω^p and $\chi_{\max}$ are functions of β [44]. The quality of the Kohlrausch fits can be seen in Figs. 7 and 16. For frequencies $\omega\tau<1$ the Kohlrausch fit, the numerical results, and the Debye fit are very close to each other. The upper part of the α peak can be fitted well by the Kohlrausch law. On the high-frequency side, however, systematic deviations, increasing with increasing frequency, can be seen in general. The Kohlrausch law falls below the von Schweidler asymptote because of

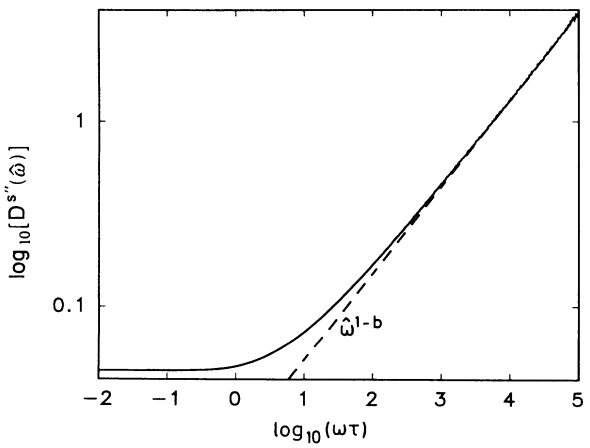

FIG. 15. Double-logarithmic plot of the normalized self-diffusion function $D^s(\hat{\omega})/(a^2/\tau)$. The high-frequency asymptote proportional to $\hat{\omega}^{1-b}$ is included.

$\beta_q>b$. The q-dependent variation of the stretching observed in ω_p and Σ_q of course translates into a q variation of β_q. Figure 17 shows that β_q changes by roughly 20% around the primary peak of S_q. The Kohlrausch relaxation time τ_q^K also changes drastically by a factor of 6 at the peak q_p. In the tagged-particle motion, β_q varies monotonically from $\beta=0.99$ at $q=1.5/a$ to $\beta=0.58$ at $q=15/a$, see Fig. 18. The Kohlrausch relaxation time varies by two orders of magnitude in the wave-vector range $q=1.5/a$ to $15/a$.

A trend in the quality of the Kohlrausch fit is found. For large q the fits approximate the coherent and incoherent susceptibilities χ_q'' and $\chi_q''^s$ better. β_q comes closer to b and takes the rather constant value 0.56 ± 0.01 for $qa>20$. The conjecture for the wave-vector dependence of τ_q^K [41], namely $\tau_q^K\approx(f_q^c/h_q)^{1/2}$, becomes valid within insignificant errors for $qa>20$. This relation would be valid if the von Schweidler law were the short-time expansion of a Kohlrausch law with $\beta=b$. At the structure peak, however, this estimate lies a factor of 4 above the observed value. Even at the cutoff $q=q_{\max}$, however, the Kohlrausch law still deviates from the numerical results by more than numerical error.

The Kohlrausch fits to the memory functions are of intermediate and rather q-independent quality. Two, even for $q\neq0$, representative examples have been included in Figs. 10 and 14. Because of the almost constant width of the resonances in $m_q''(\hat{\omega})$, $m_q''^s(\hat{\omega})$, and $m_q''^t(\hat{\omega})$, the values of the Kohlrausch exponent are close to $\beta_q=0.58\pm0.03$ for all wave vectors.

That the Kohlrausch law is an appropriate but not exact fitting function can be seen by transferring the frequency-dependent functions back into time. The Kohlrausch fits, with the parameters obtained from the frequency-dependent functions, describe the decay of $\Phi_q(\hat{t})$ rather well, except for the initial von Schweidler regime (see Fig. 19). An extrapolation to $\hat{t}=0$ using the

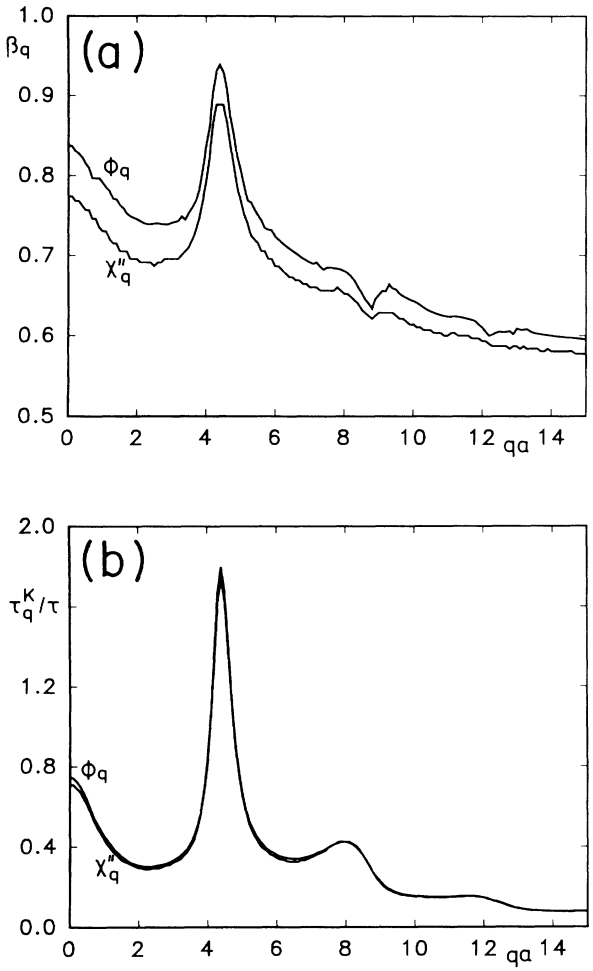

FIG. 17. (a) Kohlrausch exponents β_q for the coherent density fluctuations. The upper curve was obtained from the slope of the correlators at the point of inflection in time space; the lower curve is calculated from the peak width in the corresponding susceptibility. (b) Kohlrausch relaxation times τ_q^K of the coherent density fluctuations in units of the α scaling time τ. The upper curve is determined by the point of inflection of the correlators, the lower curve is calculated from the peak positions in the corresponding susceptibilities.

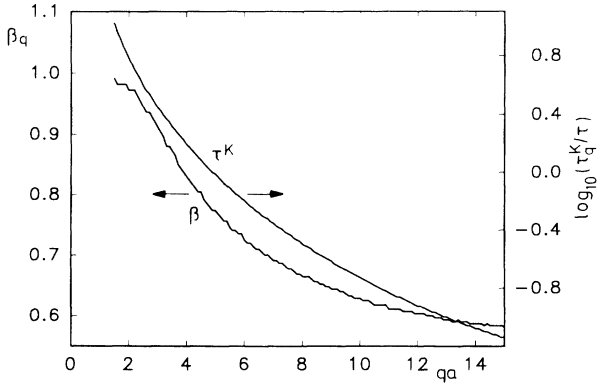

FIG. 18. Kohlrausch exponent β_q and relaxation time τ_q^K for the incoherent self-motion and obtained from $\chi_q''^s(\hat{\omega})$. Due to the strong variation of τ_q^K a logarithmic plot is chosen for it.

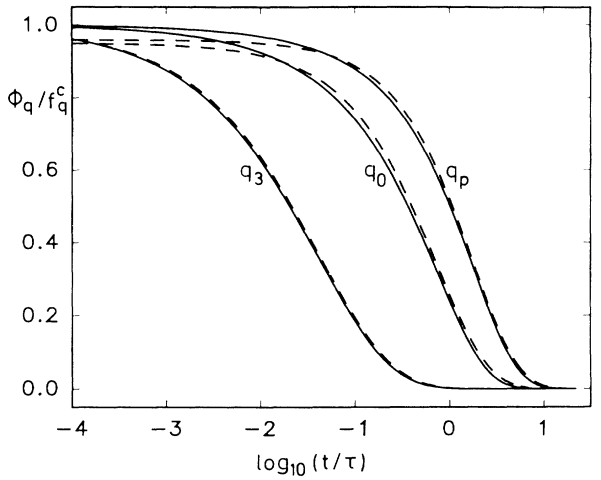

FIG. 19. Normalized correlators $\Phi_q(\hat{t})/f_q^c$ with the corresponding Kohlrausch fits are shown. The Kohlrausch-fit parameters were determined from the peaks in the susceptibilities. The shown fits for the wave vectors $q=q_3$, q_0, and q_p from left to right are representative for the quality of the fits in time space achievable with Kohlrausch parameters from frequency space.

Kohlrausch function underestimates the exact α relaxation strength f_q^c by up to 5%. A real measurement of the time-dependent function $\Phi(\hat{t})$ in a finite time window limited by the short-time β-dynamics corrections and long-time noise problems will result in rather close-fit parameters. In the familiar Kohlrausch plot $\log_{10}[-\ln\Phi_q(\hat{t})/f_q^c]$, as a function of $\log_{10}t$, an observation of the curvature of the correlators requires rather exact data and a large time window. Figure 20 shows this for $q=q_p$ and $qa=20$.

A different way of parametrizing the α stretching and the shift of relaxation times is suggested by the following property of the Kohlrausch function $\Phi^K(t)=f^K e^{-(t/\tau)^\beta}$.

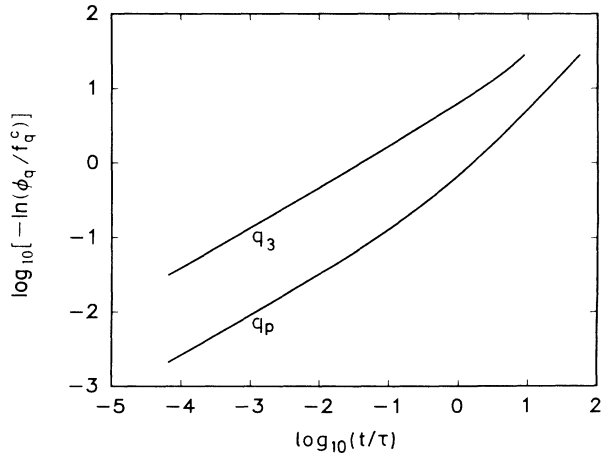

FIG. 20. Kohlrausch plot of the normalized density correlators $\Phi_q(\hat{t})/f_q^c$ for the two wave vectors $q=q_3$ (upper) and $q=q_p$ (lower curve). In a plot of $\log_{10}\{-\ln[\Phi_q(t/\tau)/f_q^c]\}$ vs $\log_{10}(t/\tau)$, Kohlrausch functions result in straight lines.

At $t=\tau$ the second derivative with regard to $\ln t$ vanishes: $(\partial^2/\partial \ln(t)\Phi^K(t)|_{t=\tau}=0$. The first derivative is proportional to β: $(\partial/d\ \ln t)\Phi^K(t)|_{t=\tau}=f^K\beta e^{-1}$. The value of the Kohlrausch function at $t=\tau$ is of course $\Phi^K(t=\tau)=f^K e^{-1}$. These two derivatives characterize the stretching and this shift of the α process via τ_q^Σ and Σ_q, as defined above. They are compared to the corresponding values obtained from the susceptibilities in Fig. 11. The values of τ_q^Σ obtained with this procedure only deviate little from the peak-position values. The stretching at τ_q^Σ is smaller than the one obtained from the peak width in χ'' due to the change from the fractal short-time asymptote to the small-frequency normal behavior. Consequently, the Kohlrausch parameters β_q obtained from Σ_q lie systematically between 2% for large q and 9% at $q=q_p$ above the values from the susceptibilities. This corroborates the statements concerning the equality of the Kohlrausch fits and can serve as an error estimate. Kohlrausch curves using the parameters from the inflection points deviate more strongly from the correlators for $t/\tau \ll 1$ than the fits in Fig. 19. Therefore, we use the values obtained from the susceptibilities when comparing with experimental least-squares Kohlrausch fits to the time-dependent correlators. The values $\beta_{q_p}=0.89$ at the peak of S_q and $\beta_{\tilde{q}}=0.74$ at $\tilde{q}=\frac{6}{7}q_p=3.8/a$ are close to the results of Bengtzelius for a Lennard-Jones system at the glass transition. He reports $\beta_{q_p}=0.88$ and $\beta_{\tilde{q}}=0.68$ [21].

Another fit formula for the α relaxation is the Cole-Davidson law $\chi^{\rm CD}(z)=\chi_0/(1-iz\tau^{\rm CD})^\alpha$ [45]. $\alpha \le 1$ is responsible for the asymmetric stretching of $\chi''(\hat{\omega})$. If the Cole-Davidson law were valid, the Cole-Davidson parameter would be equal to the von Schweidler exponent $\alpha=b$. The fitting procedure again calculates α from the width of the resonance peak, takes τ from the peak position, and takes χ_0 from the peak height. Figure 21 shows that fits of varying quality are obtained. For some wave vectors the Cole-Davidson fit is superior to the Kohlrausch fit; for others the opposite situation is observed. Except for small q, $qa \le 1.5$, and close to the primary peak $4.0 \le qa \le 5.5$, the fitted Cole-Davidson parameters lie below the von Schweidler exponent $\alpha < b$. Therefore for most q values the fits lie above the spectrum at large frequencies. The Cole-Davidson fit is excellent but not exact for those wave vectors q where the fitted α equals b; for example, at $qa=1.2$, α taken from the width of the α peak is 0.53.

Only recently has it been observed that with a very special scaling procedure dielectric loss measurements of the α relaxation for a variety of systems can be scaled onto one single scaling function [33]. This scaling property was reported to hold for different temperatures, different materials, and even for systems where the simple time-temperature superposition principle was violated. A plot of the scaled variable $Y_q=(1/\hat{w}_q)\log_{10}[\chi_q''(\hat{\omega})/f_q^c\omega/\omega_q^p]$ as a function of the scaled frequency $X_q=(1/\hat{w}_q)(1+1/\hat{w}_q)\log_{10}(\omega/\omega_q^p)$ should collapse all different curves onto one master function. Here $\hat{w}_q$ is the full width of the α resonance normalized by the Debye result, $\hat{w}_q=w_q/1.39$. The susceptibilities $\chi_q''(\hat{\omega})$ for

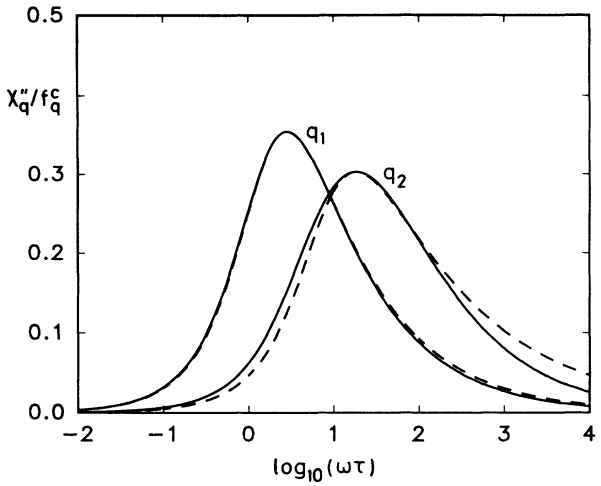

FIG. 21. Normalized susceptibilities $\chi_q''(\hat{\omega})/f_q^c$ compared to Cole-Davidson fits (dashed curves). The left susceptibility for wave vector $q=q_1$ exemplifies a good fit, where $\alpha^{\rm CD}=0.49$ is close to the von Schweidler exponent b; the curves on the right-hand side for $q=q_3$ exemplify the strong deviation of the Cole-Davidson fit if $\alpha^{\rm CD}=0.35$ is much smaller than b.

$q=q_0$, q_1, q_p, q_2, and q_3 do not reduce to one master function if plotted as specified (see Fig. 22). Neither the deviations for $X<0$, where Y does not go to the same value for all q nor the fanning out of the correlators for $X>0$ can be explained by numerical errors. In Fig. 23 for $q=q_p$ the susceptibility and the fitted Kohlrausch and Cole-Davidson laws are plotted in this fashion and compared to values tentatively read off from Fig. 3(b) of Ref. [33]. It can be seen that, especially for large X, the MCT correlator lies closer to the reported master function than the Kohlrausch or Cole-Davidson fits. The upward curvature of the master function for X around 4 is not reproduced by the MCT result, which gives a straight line corresponding to the von Schweidler asymptote. The

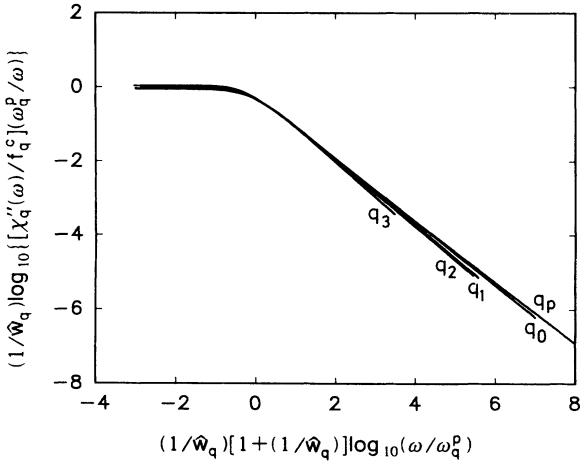

FIG. 22. Scaling plot as suggested by Dixon *et al.* [33] and mentioned in the text. The susceptibilities for the wave vectors q_3, q_2, q_1, q_0, and q_p are shown from left to right.

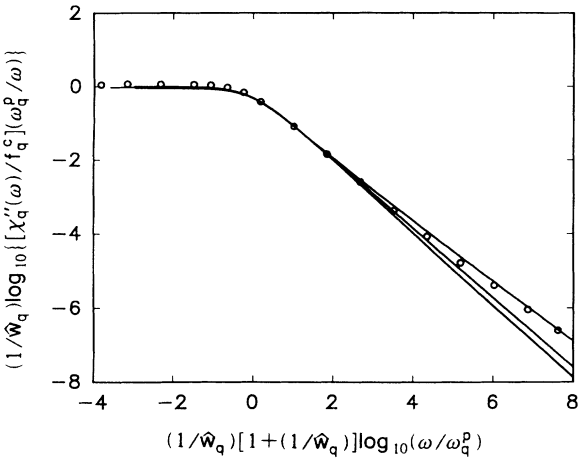

FIG. 23. Scaling plot according to Dixon *et al.* [33]. The data points are read off from their Fig. 3(b). The curves correspond to the rescaled susceptibility at $q=q_p$, the rescaled Cole-Davidson fit to this susceptibility, and the corresponding Kohlrausch fit from top to bottom at high frequencies.

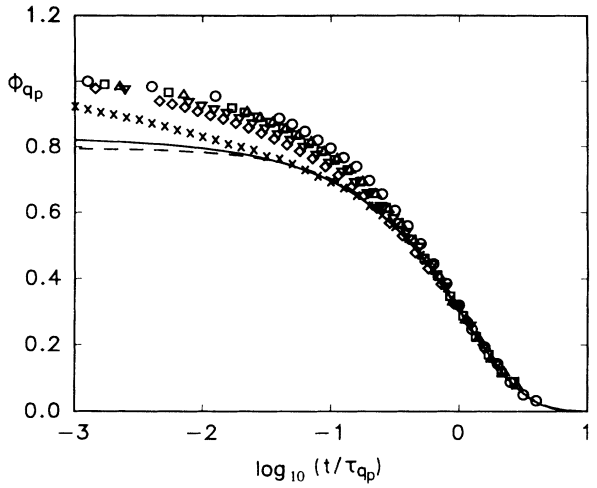

FIG. 24. α relaxation data of a colloidal suspension for wave vector at the structure peak in S_q are reproduced from Refs. [30,31]. The symbols ○, △, □, ▽, ◇, and × correspond to the packing fractions $\varphi_{\text{expt}}=0.480$, 0.494, 0.504, 0.520, 0.529, and 0.542. The critical packing fraction of this system was reported to be $\varphi^c_{\text{expt}}=0.560$ [24]. The correlator $\Phi_q(t)$ at $q=q_p$ is rescaled as explained in the text and appropriately shifted to match at $t/\tau_q=1$. The corresponding Kohlrausch fit to this correlator with $\beta_q=0.89$ is also shown as a dashed curve.

region of validity of the von Schweidler law, however, cannot be specified in general. It is possible that in $\epsilon''(\hat{\omega})$ the asymptote is only observed for much larger $X\approx 6$, where the Dixon-Nagel function flattens out again. Moreover, data from much below T_c, explicitly violating the simple α time-temperature superposition principle, have been included in the experimental scaling. Only further developments of the MCT for finite separations from the critical point, especially in the nonergodic state including activated hopping, can show whether such a curvature can be explained theoretically.

As mentioned in the Introduction, the faster β dynamics of a colloidal suspension [30] could quantitatively be fitted with the MCT results from a HSS [31]. The following observations regarding the α relaxation of $\Phi_q(t)$ at $q=q_p$ were made. (1) The time-temperature superposition principle is valid for packing fractions $\varphi\le 0.542$. The α-relaxation time varies in accordance with the MCT prediction. (2) Deviations of the curves from the α master function at short times $t/\tau\ll 1$ are explained by the β dynamics. (3) The exponent parameter $\tilde{\lambda}=0.758$ taken from [27] cannot be varied by more than 4% without destroying the agreement between theory and data. (4) The β analysis gives $\tilde{f}^c_{q_p}=0.83$ and $\tilde{h}_{q_p}=0.36$ [46]. A -5% error in the first and a $+20\%$ error in the second quantity, relative to the theoretical values [3,27], had to be accepted for the analysis. (5) The von Schweidler asymptote can fit the α decay down to $\Phi_{q_p}(t)\approx\tilde{f}^c_{q_p}e^{-1}=0.3$.

The reported value of $\tilde{\lambda}=0.758$ is very comparable to our value of $\lambda=0.766$. The small difference from the value from [27] is due to different numerical separations from the transition point. In Fig. 6 of Ref. [31] data for six different packing fractions below the experimental critical packing fraction $\varphi^c=0.560$ and a Kohlrausch fit with $\beta_{q_p}=0.88$ were shown. Figure 24 reproduces the same set of data. The above-mentioned Kohlrausch fit fits the data for $t/\tau_{q_p}\ge 1$. Our calculated correlator $\Phi_{q_p}(\hat{t})$ scaled by $\tilde{f}^c_{q_p}/f_{q_p}$ and appropriately shifted in order to match at $t/\tau_{q_p}=1$ describes the data in the regime $t/\tau_{q_p}\ge 1$, where scaling is obeyed. For $\log_{10}(t/\tau_{q_p})\ge -1.2$ the experimental data closest to the critical packing fraction are also reproduced. Φ_{q_p} has the exact critical amplitude h_{q_p}. This eliminates the large error in h_{q_p}, which was accepted in [31] in order to explain more than 50% of the α decay with the von Schweidler asymptote. In Fig. 5 it was shown that such fits to the exact results can determine the von Schweidler exponent rather well. The relative difference between our b and the value $\tilde{b}(\tilde{\lambda})=0.545$ is less than 2.5%, although large errors in the critical amplitude $\tilde{h}_{q_p}$ occur. The β dynamics accounts for the deviations of the data from the α master curve for short times, as shown in Ref. [31]. There also can be a discussion of the theoretical overestimate of the $f^c_{q_p}$ value be found. β dynamics can only explain deviations of the correlators from the α master curve if the data points lie above the α curve. The Kohlrausch fit shown as a dashed line in Fig. 24 is therefore superior to the one of Fig. 6 in Ref. [31]. In view of experimental tests of MCT predictions it should be pointed out that the superior Kohlrausch fit leads to an error in the estimated Debye-Waller factor f^c_q. As discussed in context with Fig. 19 an extrapolation to f^c_q using this Kohlrausch fit leads to an even smaller value.

V. CONCLUSION

The microscopic mode-coupling theory of the α relaxation qualitatively reproduces the experimentally known

features of the α dynamics of supercooled simple liquids. Especially, an asymmetrically stretched shape of the spectra caused by the von Schweidler law is found. The Kohlrausch law can be used for all wave vectors as a reasonable fit. The quality of the fit improves for large wave vectors. However, for all curves there are systematic deviations from the Kohlrausch law. The Kohlrausch exponent β_q and relaxation time τ_q^K vary with wave vectors and are different for different quantities. In the coherent density correlators, β_q varies strongly around the primary peak of the structure factor. Also there is no obvious connection between the Kohlrausch exponent of the modulus and the related correlator. These findings are in qualitative agreement with experiments. In neutron-scattering experiments on polybutadiene [10] a wave-vector dependence of the exponent β_q and of the relaxation time τ_q^K was found. Lindsey, Patterson, and Stevens [47] report different β for polarized and depolarized light scattering. The Cole-Davidson law also provides reasonable fits to our data. Like the Kohlrausch law it also does not describe the data exactly. It depends on the wave vector whose formula provides a better fit. The only common feature of the spectra is the same von Schweidler law for the high-frequency wing of the susceptibilities. It is also seen in the short-time expansion of the time-dependent functions. The numerical solutions, however, show that its range of validity is in general very small in a hard-sphere system. For possible future tests of the MCT it is important to note that an unbiased fit of the short-time $t/\tau < 1$ side of the α relaxation gives a von Schweidler exponent very close to the exact one.

Our numerical work using the MCT factorization approximation gives reasonable results even in the hydrodynamic range $q \to 0$. For example, the Stokes-Einstein relation is verified by combining rather independent results for the tagged particle and the stress correlation functions.

With our results for the intermediate scattering function at the first peak of the structure factor we can quantitatively explain experiments on colloidal hard-sphere systems [30]. This completes the β-relaxation analysis of the same set of data done by Götze and Sjögren [31]. The experimentally observed slow relaxation for $q = q_p$ of a hard-sphere system at the liquid-to-glass transition is in quantitative agreement with the *ab initio* MCT predictions. Our work provides a variety of detailed results on the α dynamics of hard-sphere colloids. If the experiments on these systems could be extended to a larger set of wave vectors, a rather detailed test of the relevance of the MCT could be conducted.

ACKNOWLEDGMENTS

We cordially thank Professor W. Götze for introducing us to the glass-transition problem and for his stimulating interest in our work. We thank Professor W. Götze and Dr. L. Sjögren for a critical reading of the manuscript.

[1] J. Wong and C. A. Angell, *Glass: Structure by Spectroscopy* (Dekker, New York, 1976).
[2] E. Leutheusser, Phys. Rev. A **29**, 2765 (1984).
[3] U. Bengtzelius, W. Götze, and A. Sjölander, J. Phys. C **17**, 5915 (1984).
[4] T. R. Kirkpatrick, Phys. Rev. A **31**, 939 (1985).
[5] S. P. Das and G. F. Mazenko, Phys. Rev. A **34**, 2265 (1986).
[6] W. Götze, in *Liquids Freezing and the Glass Transition,* edited by D. Levesque, J. P. Hansen, and J. Zinn-Justin (North-Holland, Amsterdam, 1991), p. 287.
[7] B. Kim and G. F. Mazenko, Adv. Chem. Phys. **78**, 129 (1991).
[8] W. Götze, Philos. Mag. B **43**, 219 (1981); in *Recent Developments in Condensed Matter Physics,* edited by J. T. Devreese (Plenum, New York, 1981), Vol. 1.
[9] S. F. Edwards and P. W. Anderson, J. Phys. F **5**, 965 (1975).
[10] B. Frick, B. Farago, and D. Richter, Phys. Rev. Lett. **64**, 2921 (1990).
[11] E. Bartsch, M. Kiebel, H. Sillescu, and W. Petry, Ber. Bunsenges, Phys. Chem. **93**, 1252 (1989); W. Petry, E. Bartsch, F. Fujara, M. Kiebel, H. Sillescu, and B. Farago, Z. Phys. B **83**, 175 (1991).
[12] L. Sjögren, in *Basic Features of the Glassy State,* edited by J. Colmenero and A. Alegria (World Scientific, Singapore, 1990), p. 137.
[13] L. Sjögren, J. Phys. Condensed Matter **3**, 5023 (1991).
[14] F. Mezei, Phys. Scr. **T19**, 363 (1987); F. Mezei, W. Knaak, and B. Farago, Phys. Rev. Lett. **58**, 571 (1987); F. Mezei, in *Dynamics of Disordered Materials,* edited by D. Richter, A. J. Dianoux, W. Petry, and J. Teixeria (Springer, Berlin, 1989), p. 164.
[15] J. N. Roux, J. L. Barrat, and J. P. Hansen, J. Phys. Condensed Matter **1**, 7171 (1989); J. L. Barrat, J. L. Roux, and J. P. Hansen, Chem. Phys. **149**, 197 (1990).
[16] G. F. Signorini, J. L. Barrat, and M. L. Klein, J. Chem. Phys. **92**, 1294 (1990).
[17] W. Götze and L. Sjögren, Z. Phys. B **65**, 415 (1987).
[18] M. Fuchs, W. Götze, I. Hofacker, and A. Latz, J. Phys. Condensed Matter **3**, 5047 (1991).
[19] J. Bosse and J. S. Thakur, Phys. Rev. Lett. **59**, 998 (1987); J. S. Thakur and J. Bosse, J. Non-Cryst. Solids **117/118**, 898 (1990).
[20] J. L. Barrat and A. Latz, J. Phys. Condensed Matter **2**, 4289 (1990).
[21] U. Bengtzelius, Phys. Rev. A **34**, 5059 (1986).
[22] P. N. Pusey, in *Liquids Freezing and the Glass Transition,* edited by D. Levesque, J. P. Hansen, and J. Zinn-Justin (Elsevier, Amsterdam, 1991), p. 763; W. van Megen and I. Snook, Adv. Colloid Interface Sci. **21**, 119 (1984).
[23] P. N. Pusey and W. van Megen, Nature **320**, 340 (1986); P. N. Pusey and W. van Megen, in *Physics of Complex and Supermolecular Fluids,* edited by S. A. Safran and N. A. Clark (Wiley, New York, 1987).
[24] P. N. Pusey and W. van Megen, Phys. Rev. Lett. **59**, 2083 (1987).
[25] P. N. Pusey and W. van Megen, Ber. Bunsenges. Chem. **94**, 225 (1990).
[26] L. V. Woodcock and C. A. Angell, Phys. Rev. Lett. **16**,

1129 (1981).
[27] J. L Barrat, W. Götze, and A. Latz, J. Phys. Condensed Matter **1**, 7163 (1989).
[28] U. Bengtzelius, Phys. Rev. A **33**, 3433 (1986).
[29] W. Götze, Z. Phys. B **60**, 195 (1985).
[30] W. van Megen and P. N. Pusey, Phys. Rev. A **43**, 5429 (1991).
[31] W. Götze and L. Sjögren, Phys. Rev. A **43**, 5442 (1991).
[32] S. P. Das, Phys. Rev. A **42**, 6116 (1990).
[33] P. K. Dixon, L. Wu, S. R. Nagel, B. D. Williams, and J. P. Carini, Phys. Rev. Lett. **65**, 1108 (1990).
[34] J. P. Hansen and I. R. McDonald, *Theory of Simple Liquids,* 2nd ed. (Academic, London, 1986).
[35] W. Götze and M. Lücke, Phys. Rev. B **13**, 3825 (1976).
[36] W. Hess, J. Phys. A **14**, L145 (1981).
[37] W. Hess and R. Klein, J. Phys. A **13**, L5 (1980); B. Cichocki and W. Hess, Physica **141A**, 475 (1987).
[38] W. Götze, in *Amorphous and Liquid Materials,* edited by E. Lüscher (Nijhoff, Dordrecht, 1987).
[39] W. Götze, Z. Phys. B **56**, 139 (1984).
[40] M. Fuchs, W. Götze, and A. Latz, Chem. Phys. **149**, 185 (1990).
[41] L. Sjögren and W. Götze, in *Dynamics of Disordered Materials,* edited by D. Richter, A. J. Dianoux, W. Petry, and J. Teixeira (Springer, Berlin, 1989), p. 18.
[42] B. V. Gnedenko and A. N. Kolmogorov, *Limit Distributions for Sums of Independent Random Variables* (Addison-Wesley, Reading, MA, 1954).
[43] W. Götze and L. Sjögren (unpublished).
[44] C. P. Lindsey and G. D. Patterson, J. Chem. Phys. **73**, 3348 (1980).
[45] D. W. Davidson and R. H. Cole, J. Chem. Phys. **19**, 1484 (1951).
[46] The numerical value $\tilde{h}_{q_p}=0.36$ was reported as $\tilde{h}_{q_p}=0.48$ in Ref. [31] due to a different system of units.
[47] C. P. Lindsay, G. D. Patterson, and J. R Stevens, J. Polymer Sci. Poly. Phys. Ed. **17**, 1547 (1979).